Makara Journal of Science

Volume 23
Issue 2 *June*

Article 3

6-20-2019

Extraction of "Quercetin-Rich" Red Onion Skin with Acetone and Chemical Modification using Aromatic Diazonium Salts

Gervais Manizabayo
Department of Pure and Industrial Chemistry, University of Port Harcourt, Nigeria

Uche John Chukwu
Department of Pure and Industrial Chemistry, University of Port Harcourt, Nigeria,
uche.chukwu@uniport.edu.ng

Ovi Julius Abayeh
1. Department of Pure and Industrial Chemistry, University of Port Harcourt, Nigeria. 2. World Bank Africa Centre of Excellence for Oilfield Chemicals Research, University of Port Harcourt, Nigeria.

Recommended Citation

Manizabayo, Gervais; Chukwu, Uche John; and Abayeh, Ovi Julius (2019) "Extraction of "Quercetin-Rich" Red Onion Skin with Acetone and Chemical Modification using Aromatic Diazonium Salts," *Makara Journal of Science*: Vol. 23 : Iss. 2 , Article 3.
DOI: 10.7454/mss.v23i2.11045
Available at: https://scholarhub.ui.ac.id/science/vol23/iss2/3

Makara Journal of Science, 23/2 (2019), 79-86
doi: 10.7454/mss.v23i2.11045

Extraction of "Quercetin-Rich" Red Onion Skin with Acetone and Chemical Modification using Aromatic Diazonium Salts

Gervais Manizabayo[1], Uche John Chukwu[1*], and Ovi Julius Abayeh[1, 2]

1. Department of Pure and Industrial Chemistry, University of Port Harcourt, Nigeria
2. World Bank Africa Centre of Excellence for Oilfield Chemicals Research, University of Port Harcourt, Nigeria

[*]*E-mail: uche.chukwu @uniport.edu.ng*

Received October 23, 2018 | Accepted May 15, 2019

Abstract

The extraction of "quercetin-rich" red onion skin (red onion skin extract [ROSE]) using acetone and chemical modification with aromatic diazonium salts of aniline (AmROSE), 2-aminophenol (APmROSE), and 2-aminobenzoic acid (ABmROSE) were carried out in this study. The effects of the particle diameter of red onion skin (ROS), volume of the solvent, and percentage of acetone in the solvent mixture on the extraction yield were investigated. The solubility, color, melting point, and functional groups present in ROSE before and after modification were also analyzed. The extraction of ROS using an aqueous solvent of 50% acetone gave the highest percentage extraction yield. In addition to the C=O, OH, C-O-C, and C-O-H functional groups that were present in both unmodified ROSE (UROSE) and modified ROSE, Infrared spectra results revealed that all the modifications (AmROSE, APmROSE, and ABmROSE) showed the presence of N=N and C-N of aromatic azo compounds at 1512–1496 and 1288–1256 cm^{-1}, respectively. The three modifications were also found to be more soluble than UROSE in all the solvents. The melting point of UROSE and its modifications was within the range of 78 °C–105 °C, which was lower than that of commercial quercetin dehydrate P-Q (300 °C–310 °C).

Keywords: acetone, diazonium salt, extraction, quercetin, red onion skin

Introduction

Onions are regarded as one of the most widely consumed vegetables across the globe [1]. However, the outer parts of onions, which are commonly known as "onion skins," are usually discarded as waste and may be a nuisance to the environment especially when improperly disposed. Red onion skin (ROS) contains the highest concentration of "quercetin" [2] and other polyphenolic compounds [3]. In addition to its anti-oxidative, anti-apoptosis, and anti-inflammatory properties [4], quercetin has excellent metal chelation properties similar to other flavonoids [5-9]. The metal chelating property of quercetin is attributed to the presence of five hydroxyl groups at positions 3, 5, 7, 3', and 4' and a carbonyl group at position 4 (Figure 1). The metal chelation properties of quercetin can be improved by introducing azo (N=N) functional groups in the structure through a coupling reaction with an aromatic diazonium salt. This paper reports the extraction of "quercetin-rich" ROS and the modification of ROS extract (ROSE) using aromatic amines through diazotization and coupling processes, respectively. The proposed reaction mechanism and products for the synthesis of diazonium salt and coupling with "quercetin-rich" ROSE are shown in Schemes 1 and 2, respectively.

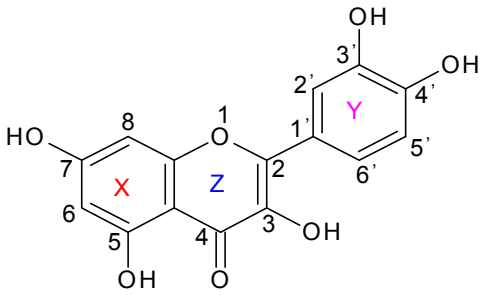

Figure 1. Structure of Quercetin

Materials and Methods

Collection and pretreatment of ROS. ROS was collected from an oil mill and fruit garden markets in Port Harcourt, Nigeria. The skins were carefully selected, thoroughly washed with distilled water, air dried at ambient temperature, and pulverized into powder form using an electric grinder. The pulverized

ROS was sieved to generate ROS particles of different diameters (500, 355, 250, 180, and 125 µm).

Extraction of ROS.

A: Effect of solvent volume on the extraction yield. The effect of the solvent volume on the extraction yield was investigated by soaking 20 g of 500 µm diameter ROS in 150, 200, 250, 300, 350, and 400 mL of 50% acetone for 48 h at room temperature. The extract was filtered and concentrated in a water bath set at 50 °C. ROSE was weighed, and the percentage extraction yield was calculated and plotted against the volume of the solvent (Figure 2).

B: Effect of ROS particle diameter on the extraction yield. The effect of ROS particle diameter on the percentage extraction yield was evaluated by soaking 20 g of 500 µm diameter ROS into 200 mL of 50% acetone solvent for 48 h. Subsequently, the solvent soluble extracts were then filtered and concentrated in a water bath set at 50 °C. The same procedure was followed for the extraction of 355, 250, 180, and 125 µm diameter ROS. The dried ROSE was weighed, and the percentage extraction yields were calculated and plotted against ROS size (Figure 3).

C: Effect of percentage of acetone in the solvent mixture on the extraction yield. The effect of the percentage (%) of acetone in the solvent mixture on the extraction yield was determined by soaking 20 g of 355 µm diameter ROS into 300 mL of 100% acetone, 75% acetone, 50% acetone, 25% acetone, and 0% acetone (100% water). The extract was filtered and concentrated in a water bath set at 50 °C until the solvent was fully evaporated. The dried extract was weighed, and the percentage of extraction yields was calculated and plotted against the acetone percentage in the solvent mixture (Figure 4).

Modification of ROSE.

ROSE was modified using three aromatic diazonium salts, namely, benzenediazonium chloride, 2-hydroxybenzenediazonium chloride, and carboxybenzenediazonium chloride. These salts were synthesized by the diazotization reaction of aniline, 2-aminophenol, and 2-aminobenzoic acid (Scheme 1).

Synthesis of diazonium salts. The following procedure was followed to synthesize the three diazonium salts:. Approximately 1 mL (0.01 mol) of aniline, 1.09 g (0.01 mol) of 2-aminophenol, and 1.37 g (0.01 mol) of 2-aminobenzoic acid were each dissolved into 45 mL of distilled water in three different 250 mL beakers labeled A, B, and C, respectively. To each beaker, 12 mL of 11.4 M hydrochloric acid was slowly added while stirring. The resulting solutions were cooled in an ice bath at 0 °C–5 °C. To each of the aromatic amine solutions at 0 °C–5 °C, 5 mL of cold $NaNO_2$ (0.01 mol, 0.7 g) was added dropwise while stirring at a constant rate. The reaction mixtures were then stirred for another 2–3 min. The resulting solutions were benzenediazonium chloride (beaker A), hydroxybenzenediazonium chloride (beaker B), and carboxybenzenediazonium chloride (beaker C).

The reaction equation for the synthesis of the three diazonium salts is shown in Scheme 1.

Preparation of modified ROSE (AmROSE, APmROSE, and ABmROSE). An alkaline solution of ROSE was first prepared by dissolving 3.02 g of ROSE into 30 mL of 10% sodium hydroxide solution in a 250 mL beaker. The resulting solution was cooled in an ice bath at 0 °C–5 °C. The first modification, namely, aniline-modified ROSE (AmROSE), was prepared by slowly adding benzenediazonium chloride solution to the alkaline solution of ROSE while stirring at a constant rate. The reaction mixture was stirred for another 15 min to ensure completion of the reaction. The resulting precipitate was filtered using a suction filtration apparatus, washed with a small amount of cold water, and dried at ambient temperature for 5 days.

The same procedure was followed for the synthesis of 2-aminophenol-modified ROSE (APmROSE) and 2-aminobenzoic acid-modified ROSE (ABmROSE). Scheme 2 shows the proposed reaction mechanism and products for the coupling reaction between "quercetin-rich" ROSE and diazonium salts.

Melting point and solubility study of UROSE, AmROSE, APmROSE, and ABmROSE in different solvents. The solubility test was carried out by dissolving 0.01 g of the sample in test tubes containing 5 mL of (i) water, (ii) methanol, (iii) ethanol, (iv) acetone, (v) ethyl acetate, (vi) hexane, and (vii) benzene. The test tubes were shaken for 1–2 min, and the solubility of each of the samples was observed and recorded. The results for the solubility test are presented in Table 1.

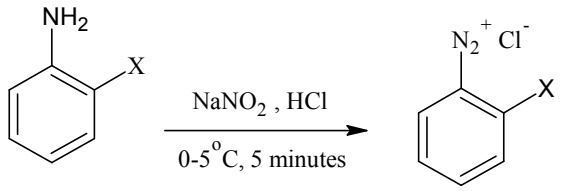

Where, X= H for Aniline

X=OH for 2-aminophenol

X=COOH for 2-aminobenzoic acid

Scheme 1. General Equation for the Synthesis of Diazonium Salts from Aniline, 2-aminophenol, and 2-aminobenzoic acid

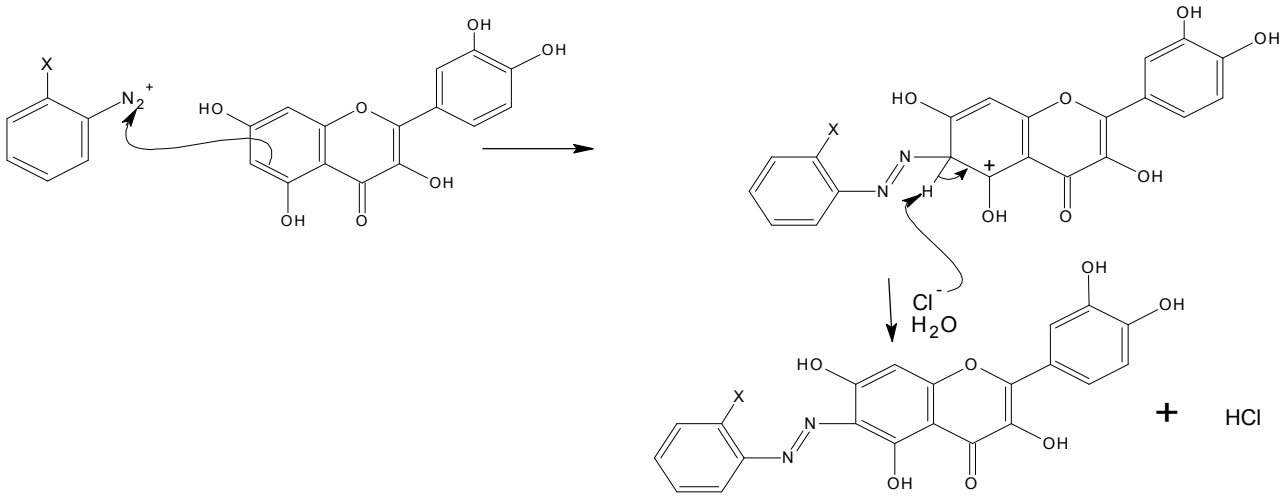

Further substution may result into the formation of the products shown below.

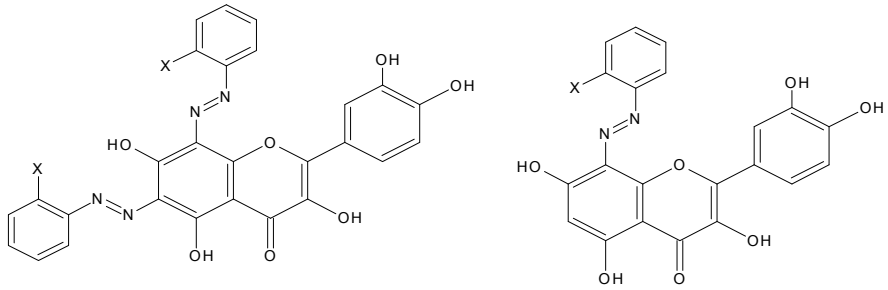

Where X=H for benzenediazonium chloride; X=OH for *p*-hydrobenzenediazonium chloride ; X=COOH for *p*-carboxybenzenediazozium chloride

Scheme 2. Proposed Mechanism and Products Formed from the Coupling Reaction between Quercetin-rich ROSE and an Aromatic Diazonium Salt

The melting point was determined using a melting point apparatus (Model no: IA-9000), and the results are presented in Table 2.

FTIR analysis of UROSE, P-Q, AmROSE, APmROSE, and ABmROSE. Unmodified ROSE (UROSE), commercial quercetin dihydrate (P-Q), and modified ROSEs (AmROSE, APmROSE, and ABmROSE) were subjected to an FTIR spectro-photometer (Model no: FTIR-8400S) to ascertain the functional groups present. The results obtained are shown in Figure 5.

Results and Discussion

Effect of volume of the solvent, acetone percentage, and ROS particle diameter on the extraction yield. The extraction yield is dependent on the volume of the solvent, the percentage of each solvent in the solvent mixture, and the sample particle diameter. The percentage extraction yield obtained from the extraction of 20 g of 500 µm diameter ROS using different solvent volumes was observed to increase with increasing solvent volume. The extraction yield increased gradually from 2.9% at 150 mL to 12.4% at 300 mL and then sharply increased to 34.9% at 350 mL of the solvent (Figure 2). However, when the volume increased from 350 mL to 400 mL, the extraction yield increased only by 5.75%, which was lower than the 22.7% increase observed from 300 mL to 350 mL of the solvent. At 350 mL, saturation was attained for the extraction of 20 g of ROS material.

The increase in ROS particle diameter resulted in a decrease in the percentage extraction yield (Figure 3). The results indicated that the percentage extraction yield decreased from 8.8% for 125 µm ROSE to 3.7% for 500 µm ROSE. The contact surface between the sample and solvent decreased as the particle diameter of the sample increased, thereby lowering the extraction efficiency. By increasing the acetone percentage in the solvent mixture, the extraction yield gradually increased possibly due to the polarity of the solvent to attract the ROS extract, which exhibited similar bond polarity [9]. At 50% acetone/water mixture, the optimum extraction yield was achieved (Figure 4). This result was in agreement

with the findings of a previous investigation by Do *et al.* (2014), who reported the effects of extraction solvent on the total phenol content of *Limnophila aromatica* [10].

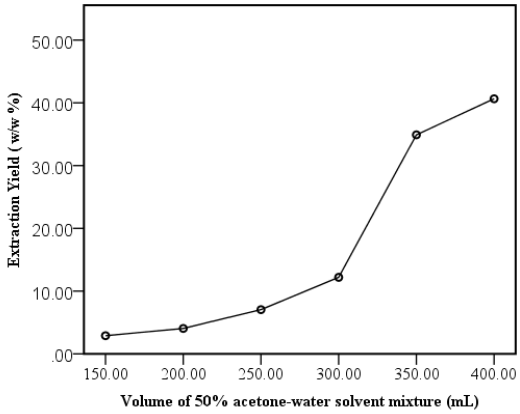

Figure 2. Effect of Volume of 50% Acetone–water Solvent Mixture on the Extraction Yield at Ambient Conditions

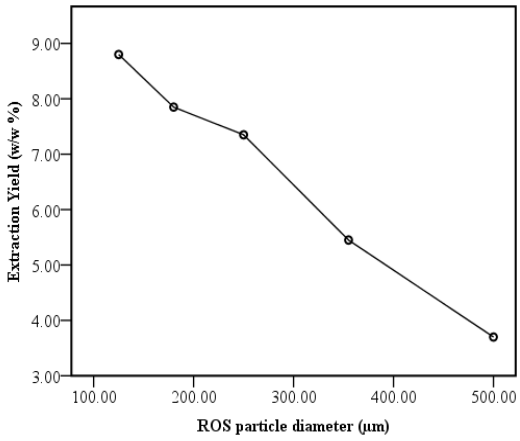

Figure 3. Effect of ROS Particle Diameter on the Extraction Yield at Ambient Conditions

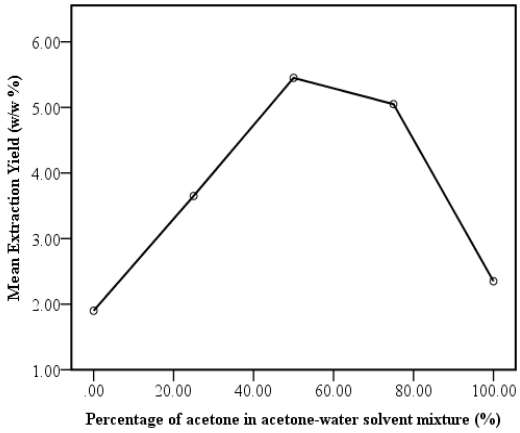

Figure 4. Effect of Acetone Percentage in the Acetone–water Solvent Mixture on the Extraction Yield at Ambient Conditions

Solubility, melting point, and color of UROSE, AmROSE, APmROSE, and ABmROSE. The results from the solubility test carried out on both UROSE and modified ROSE in water, hexane, benzene, acetone, ethyl acetate, ethanol, and methanol are presented in Tables 1 and 2. The results showed that UROSE, APmROSE, and ABmROSE were insoluble in water and hexane and partially soluble in benzene with the exception of ABmROSE. All modified ROSEs were highly soluble in ethyl acetate and soluble in acetone, ethanol, and methanol. AmROSE was found to be more soluble than UROSE, APmROSE, and ABmROSE.

Table 2 shows that the melting points of UROSE and all the modified ROSEs were lower than that of commercial P-Q. This result may be due to the presence of impurities in the extract before and after modification, as evidenced in the wide range of melting points obtained. Furthermore, the melting point of APmROSE (105 °C–110 °C) was higher than that of UROSE, AmROSE, and ABmROSE possibly because APmROSE has more O-H functional groups (Figure 6) and more hydrogen bonds than UROSE and other modifications.

Diazotization of aromatic amines and coupling with quercetin-rich ROSE. Diazotization of aromatic amines was carried out in an ice bath below 5 °C. The resulting diazonium salts were used immediately after preparation mainly because diazonium salts are highly unstable above 5 °C [11].

The synthesized diazonium salts were coupled with ROSE to produce the three modifications, namely, AmROSE, 2- APmROSE, and ABmROSE. The reaction between the diazonium salt and ROSE followed the mechanism of electrophilic aromatic substitution, where the diazonium salt served as the source of the electrophile. Given that the hydroxyl groups (OH) are ortho and/or para directing groups [12], electrophilic substitution could occur at positions 6 and 8 in ring X and 2', 5', and 6' in ring Y. However, unlike the OH groups in ring Y, the two OH groups in ring X demonstrated reinforcing or cooperative directing effects at positions 6 and 8, making ring X more reactive toward the electrophile than ring Y.

FTIR spectra of UROSE, P-Q, AmROSE, APmROSE, and ABmROSE. The FTIR spectra and key functional groups present in UROSE, commercial P-Q, AmROSE, APmROSE, and ABmROSE are presented in Figure 5 and Table 3.

The results revealed broad peaks at 3402.54, 3325.39, 3394.83, 3433.41, and 3433.41 cm^{-1}, which were possibly due to the presence of phenolic O-H stretch vibrations in UROSE, P-Q, AmROSE, APmROSE, and ABmROSE respectively [13, 14]. The strong peaks at 1643.41, 1635.23, 1635.69, 1643.41, and 1643.41 cm^{-1}

were most likely due to the presence of C=O stretching vibrations of aromatic ketone in UROSE, P-Q, AmROSE, APmROSE, and ABmROSE, respectively [15, 16].

The results also showed the presence of medium peaks at 1234.48, 1234.48, 1157.33, 1165.04, and 1165.04 cm^{-1}, which were probably due to the presence of C-O-H and/or C-O-C linkages [15, 17]. All modified ROSEs (AmROSE, APmROSE, and ABmROSE) displayed small and weak peaks at 1512.24 and 1496.81 cm^{-1}, which may be attributed to the N=N stretching vibrations of aromatic azo compounds [17-21]. Furthermore, AmROSE, APmROSE, and ABmROSE showed peaks at 1288.49, 1265.35, and 1265.35 cm^{-1}, which may be due to the presence of an aromatic C-N bond from azo compounds [15, 21, 22].

The two small and weak peaks appearing between 2850 and 2950 cm^{-1} in the FTIR spectra of UROSE, AmROSE, APmROSE, and ABmROSE were most likely due to the presence of the C-H stretching vibration of alkyls [14, 23]. The FTIR spectra of UROSE shown in Figure 5 revealed the presence of a weak peak at 1504.53 cm^{-1}, which may be attributed to aromatic C=C stretch vibration [14, 24]. The peaks at 671.25, 802.41 748.41, and 709.83 cm^{-1} were possibly due to the presence of di-substituted benzene rings in UROSE, AmROSE, APmROSE, and ABmROSE [25].

Table 1. **Solubility and Color of UROSE, AmROSE, APmROSE, and ABmROSE in Different Solvents**

Sample/ Solvent	Water	Hexane	Benzene	Acetone	Ethyl acetate	Ethanol	Methanol
UROSE	I	I	PS	S	S	S	S
AmROSE	PS	PS	S	S	HS	HS	HS
APmROSE	I	I	PS	S	HS	S	S
ABmROSE	I	I	I	S	HS	S	S

Where S: Soluble; I: Insoluble; PS: Partially soluble; HS: Highly soluble; and HI: Highly insoluble.

Table 2. Color and melting point of UROSE, AmROSE, and ABmROSE

Sample	Color	Melting point (°C)
UROSE	Reddish brown	102–105
AmROSE	Ox blood	87–91
APmROSE	Brown	105–110
ABmROSE	Dark brown	78–80
P-Q	Yellow	300–316

Table 3. Major peaks and functional groups present in UROSE, P-Q, AmROSE, APmROSE, and ABmROSE

Ligands	Peaks/Wavenumber in cm^{-1} (Functional groups)
UROSE	**3402.54** (Phenolic O-H stretch vibration)**, 2931.90 and 2862.46** (Symmetric and asymmetric C-H stretch vibration), **1643.41** (C=O stretch vibration), **1504.53** (C=C stretch vibration), **1157.33 (**C-O-H and/or C-O-C linkages), **671.25** (di-substituted benzene rings).
P-Q	**3325.39** (Phenolic O-H stretch vibration)**, 1635.69** (C=O stretch vibration)**, 1597.11** (C=C stretch vibration)**, 1234.48 (**C-O-H and/or C-O-C linkages).
AmROSE	**3394.83** (Phenolic O-H stretch vibration), **2924.18 and 2854.74** (Symmetric and asymmetric C-H stretch vibration)**, 1635.69** C=O stretch vibration)**, 1512.24** (N=N stretching vibrations)**, 1288.49** (Aromatic C-N bond), **1157.33 (**C-O-H and/or C-O-C linkages)**, 802.41** (di-substituted benzene rings).
APmROSE	**3433.41** (Phenolic O-H stretch vibration)**, 2862.46 and 2924.18** (Symmetric and asymmetric C-H stretch vibration)**, 1643.41** C=O stretch vibration)**, 1512.24** (N=N stretching vibrations)**, 1265.35** (Aromatic C-N bond), **1165.04 (**C-O-H and/or C-O-C linkages)**, 748.41** (di-substituted benzene rings).
ABmROSE	**3456.55** (Phenolic O-H stretch vibration)**, 2854.74 and 2924.18** (Symmetric and asymmetric C-H stretch vibration)**, 1635.69** C=O stretch vibration)**, 1496.81** (N=N stretching vibrations)**, 1257.63** (Aromatic C-N bond), **1157.33 (**C-O-H and/or C-O-C linkages)**, 709.83** (di-substituted benzene rings).

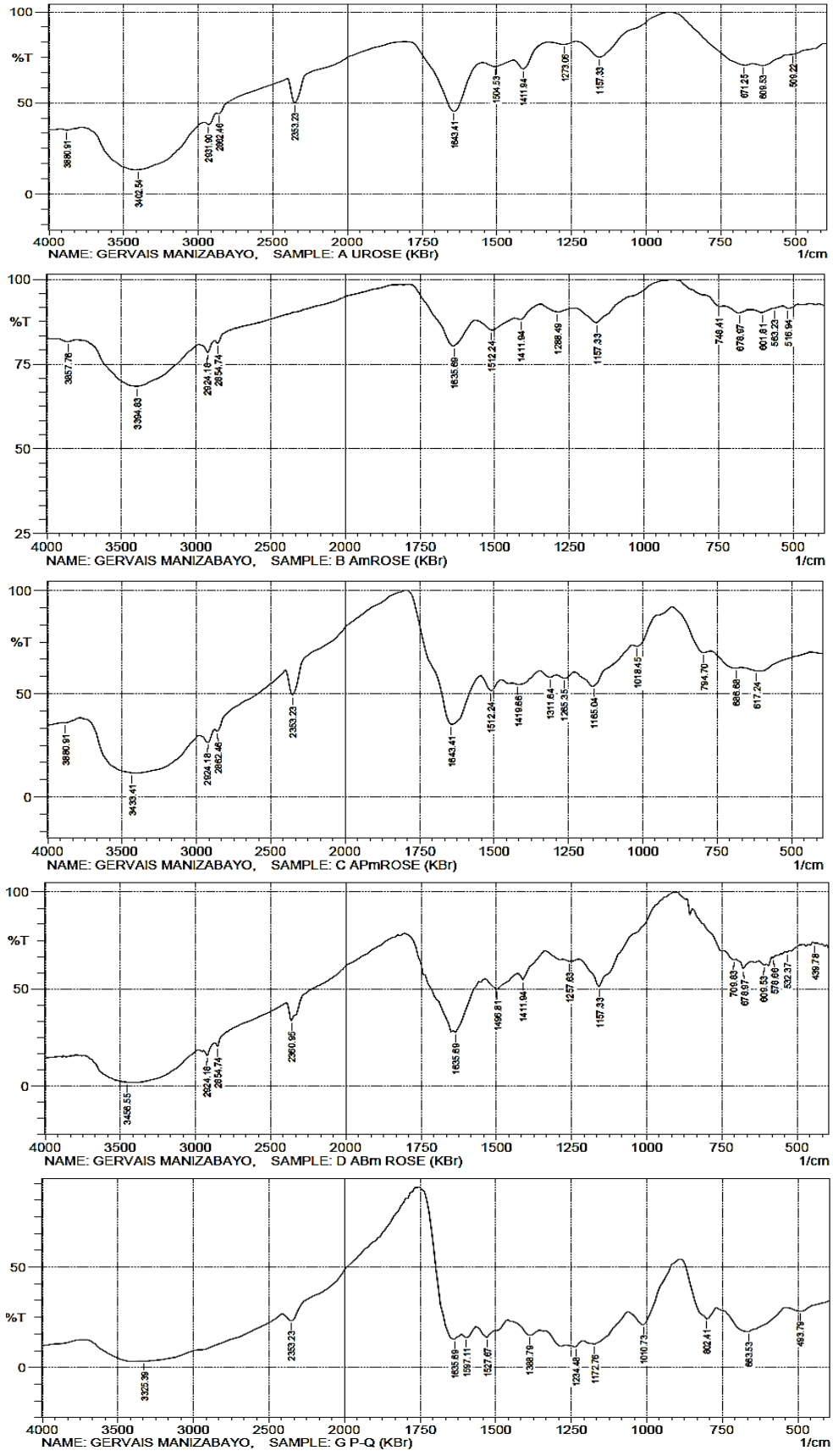

Figure 5. FTIR Spectra of UROSE, AmROSE, APmROSE, ABmROSE, and P-Q

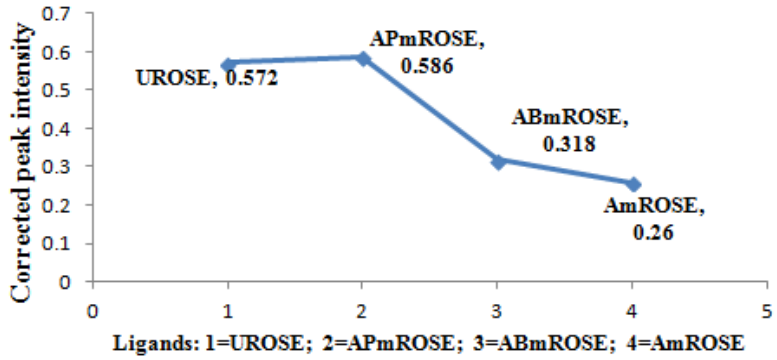

Figure 6. OH Group Peak Intensity for UROSE, APmROSE, ABmROSE, and AmROSE

Analysis of O-H peak intensity. Figure 6 shows the peak intensity for the O-H functional group present in ROSE before and after modification.

Semi-quantitatively, the O-H peak intensity increased from 0.572 for UROSE to 0.586 for APmROSE and decreased from 0.572 for UROSE to 0.318 and then to 0.26 for ABmROSE and AmROSE. The increase in the O-H peak intensity for APmROSE was probably due to the presence of the OH functional group at the ortho position of 2-aminophenol.

Conclusion

In this study, ROS was successfully extracted and modified using aromatic amines. The highest percentage extraction yield of ROSE was obtained by using an aqueous solvent system of 50% acetone. The extraction yield increased with the volume of the solvent and decreased with increasing ROS particle diameter. FTIR analysis indicated that P-Q, UROSE, and its modifications contained OH, C=O, C-O, and C=C functional groups and the di-substituted benzene ring. In addition to these functional groups, FTIR analysis revealed the presence of N=N and C-N bonds of azo compounds in all modified ROSEs (AmROSE, APmROSE, and ABmROSE). The appearance of these new functional groups and the change observed in the peak intensity of key functional groups, color, solubility, and melting point were used to justify the success of the modification process.

Funding

This research did not receive any specific grant from funding agencies in the public, commercial, or not-for-profit sectors.

Data availability

The raw/processed data required to reproduce these findings cannot be shared at this time due to legal or ethical reasons.

References

[1] Bello, M.O., Olabanji, I.O., Abdul-Hammed, M. Okunade, T.D. 2013. Characterization of domestic onion wastes and bulb (Allium cepa L.): fatty acids and metal contents. Int. Food Res. J., 20(5): 2153–2158.

[2] Sayed, H.S., Hassan, N.M.M., El, M.H.A. 2014. The Effect of Using Onion Skin Powder as a Source of Dietary Fiber and Antioxidants on Properties of Dried and Fried Noodles. Current Sci. J. 3(4): 468–475.

[3] Ifesan, B.O.T. 2017. Chemical Composition of Onion Peel (Allium cepa) and its Ability to Serve as a Preservative in Cooked Beef. Int. J. Sci. Res. Methodol. 7(4): 1–10.

[4] Alrawaiq, N.S., Abdullah, A. 2014. A Review of Flavonoid Quercetin: Metabolism, Bioactivity and Antioxidant Properties. Int. J. PharmTech Res. 6(3): 933–941.

[5] Dehghan, G., & Khoshkam, Z. 2011. Chelation of Toxic Tin (II) by Quercetin: A Spectroscopic Study. Int. Conf. Life Sci. Technol. 3: 3–5.

[6] Lakhanpal, P., Rai, D.K. 2007. Quercetin: A Versatile Flavonoid. Internet J. Med. Update. 2(2): 22–37, https://doi.org/10.4314/ijmu.v2i2.39851.

[7] Liu, Y., Guo, M. 2015. Studies on Transition Metal-Quercetin Complexes Using Electrospray Ionization Tandem Mass Spectrometry. Mol. 20: 8583–8594, https://doi.org/10.3390/molecules20058583.

[8] Symonowicz, M., Kolanek, M. 2012. Flavonoids and their properties to form chelate complexes. Biotechnol. Food Sci. 76(1): 1-7.

[9] Mohd, F.B., Razak, A., Yong, P.K., Abdullah, L. C., Yee, S.S., Yaw, T.C. 2012. The effects of Varying Solvent Polarity on Extraction Yield of Orthosiphon Stamineus Leaves. J. Appl. Sci. 12(11): 1207–1210, https://doi.org/10.3923/jas.2012.120 7.1210.

[10] Do, Q.D., Angkawijaya, A.E., Tran-Nguyen P.L., Huynh L.H., Soetaredjo F.E., Jun, Y.H. 2014. Effect of extraction solvent on total phenol content,

total flavonoid content, and antioxidant activity of Limnophila aromatica. J. Food Drug Anal. 22(3): 296–302, https://doi.org/10.1016/j.jfda.2013.11.001.

[11] Reusch, W. 2013. Electrophilic Substitution of Disubstituted Benzene Rings. Retrieved from chem.libretexts.org.

[12] Sudhir, M.S., Nadh, R.V. 2013. Diazo-coupling: A facile mean for the spectrophotometric determination of rasagiline hemitartrate. Orient. J. Chem. 29(4), 1507–1514. https://doi.org/10.13005/ojc/290429.

[13] Yılmaz, D.Ç., Pekin, M. 2017. Potentiometric and Chromatographic Study of Cu (II) and Al (III) Complexes of Quercetin. Marmara Pharm. J. 21(2): 330–337. https://doi.org/10.12991/marupj.300814.

[14] Ashokkumar, R., Ramaswamy, M. 2014. Original Research Article Phytochemical screening by FTIR spectroscopic analysis of leaf extracts of selected Indian Medicinal plants. Int. J. Curr. Microbiol. Appl. Sci. 3(1): 395–406.

[15] Shama, S.A., Kasem, M., Ali, E., Moustafa, M.E. 2014. Synthesis and Characterization and New Azo Compounds based on 2, 4-dihydroxybenzoic Acid. J. Basic Environ. Sci. 1: 76–85.

[16] Dixit, B., Patel, H., Desai D. 2007. Synthesis and application of new mordent and disperse azo dyes based on 2, 4-dihydroxybenzophenone. J. Serbia Chem. Soc. 72(2): 119–127. https://doi.org/10.2298/jsc0702119d.

[17] Jber, N.R., Abood, R.S., Al-dhaief, Y.A. 2011. Synthesis and Spectral Study of New Azo - Azomethine Dyes and its Copper (II) Complexes Derived from Resorcinol, 4-Aminobenzoyl Hydrazone and 4-Amino antipyrine. J. Al-Nahrain Univ. 14(4), 50–56. https://doi.org/10.22401/jnus.14.4.07.

[18] Nnaji, N.J.N., Okoye, C.O.B., Ezeokonkwo, M.A., Ani, J.U. 2013. Spectroscopic Characterization of Red Onion Skin Tannin and Its use as Alternative Aluminium Corrosion Inhibitor in Hydrochloric Acid Solutions. Int. J. Electrochem. Sci. 8: 1735–1758.

[19] Issam, A., Khalil, A. 2011. Synthesis and Characterization of a New Heterocyclic Azo Pigment. Sains Malaysiana, 40(7): 765–770.

[20] Mohammed, I. A., Mustapha, A. 2010. Synthesis of New Azo Compounds Based on N-(4-Hydroxyphenyl) maleimide and N-(4-Methylphenyl) maleimide. Mol. 7498–7508. https://doi.org/10.3390/molecules15107498.

[21] Patni, N., Patni, M. 2016. Pelagia Research Library. Chem. Sinica, 7(2): 93–100.

[22] Shelke, N.S., Thakare, N.S. 2016. Amino Phenolic AZO Compounds Synthesis and Bilogical Analysis. Res. J. Chem. Sci. 6(8): 36–42.

[23] Ahmed, F., Dewani, R., Pervez, M.K., Mahboob, S.J., Soomro, S.A. 2016. Non-destructive FT-IR analysis of mono azo dyes. Bulg. Chem. Commun. 48(1): 71–77.

[24] Coates, J. 2006. Interpretation of Infrared Spectra, a Practical Approach. In Encyclopedia of Analytical Chemistry. John Wiley & Sons Ltd. pp. 10815–10837.

[25] Yuen, C.W.M., Ku, S.K.A., Choi, P.S.R., Kan, C. W., Tsang, S.Y. 2005. Determining Functional Groups of Commercially Available Ink-Jet Printing Reactive Dyes Using Infrared Spectroscopy. RJTA, 9(2): 26–38, https://doi.org/10.1108/rjta-09-02-005-b004.